Efficiency Improvement of Current-Fed DAB Converter by Triangular Current Mode for Wide Voltage Applications

Hiroki Watanabe[1], Akira Tamagawa[1], and Jun-ichi Itoh[1]
1 Department of Electrical, Electronics and Information Engineering, Nagaoka University of Technology, Nagaoka, Japan
*E-mail: hwatanabe@vos.nagaokaut.ac.jp

***Abstract*—This paper proposes a control method of a Current-Fed DAB converter by Triangular Current Mode (TCM). The proposed method extends the Zero-Voltage-Switching (ZVS) range for wide input/output voltage variations. In addition, the proposed method reduces the inductor RMS current compared with the typical DAB converter. The validity of the proposed method is demonstrated by a 2-kW prototype circuit. As a result, the maximum efficiency of the Current-Fed DAB converter with the proposed method is 97.5% at rated load conditions. Moreover, the efficiency of the Current-Fed DAB converter with the proposed method is 97.2% when the input voltage is varied by 50% from the nominal condition, then the loss is reduced by 52.5% compared to that of the conventional method.**

Keywords—Current-Fed DAB converter, Zero voltage switching, Triangular Current Mode, Pulse Frequency Modulation

I. INTRODUCTION

Recently, DC micro-grid systems have been widely considered because of their high system efficiency, high compatibility to renewable energy sources, and Electric Vehicles (EVs) [1]-[2]. An isolated bidirectional DC-DC converter is often adopted as the interface converter between the DC-bus and each energy source owing to the feature of the bidirectional power flow control.

Especially, a Dual Active Bridge (DAB) converter has been considered owing to attractive advantages, e.g., 1) simple configuration, 2) galvanic isolation, and 3) low switching losses by Zero Voltage Switching (ZVS) [3]-[5]. However, it is well known that the DAB converter has a narrow high-efficiency condition because the large circulating current and the ZVS operation failure increase conversion losses when the transformer voltage ratio does not match the transformer turn ratio due to input/output voltage variations [6].

Various circuit topologies based on the DAB converter have been studied in order to solve this problem [7]-[11]. One of them is a configuration in which a multilevel circuit is applied to each bridge [12]-[14]. For example, the T-type DAB converter extends the ZVS range by generating multiple multilevel waveforms [15]. However, the number of components increases in a configuration in which a multilevel circuit is applied to each bridge.

In addition, the two-stage converter which consists of the DAB converter and the non-isolated DC-DC converter is proposed in order to solve this problem [16]. In this method, the input voltage of the DAB converter is regulated by a DC-DC converter to match the turn ratio of the transformer. Therefore, the DAB converter keeps high-efficiency operation against the input voltage variation. However, the two-stage configuration limits the conversion efficiency compared to the single-stage converter.

On the other hand, a Current-Fed DAB converter that integrates the DC-DC converter and the DAB converter has been proposed [17]-[21]. The Current-Fed DAB converter reduces the input current ripple by the series-connected boost inductor. In particular, the transformer voltage ratio is matched to the turn ratio by the voltage control. The circuit configuration of the Current-Fed DAB converter is classified into two types 1) single-leg Current-Fed DAB converter and 2) interleave Current-Fed DAB converter. Especially, the interleave Current-Fed DAB converter drastically reduces the input current ripple by the interleave control with phase-shifted carrier modulation. However, the ZVS operation of the power devices on the primary H-bridge of the Current-Fed DAB converter fails because of the boost inductor current with Continuous Current Mode(CCM). Therefore, the Current-Fed DAB converter also has the drawback for the high-efficiency operation.

In this paper, the control method of the Current-Fed DAB converter that achieves low RMS current and the improvement of the ZVS range is proposed against the input voltage variation. The originality of this paper is applying the Triangular Current Mode (TCM) to the boost inductor current. The ZVS range of the Current-Fed DAB converter is improving by applying TCM including a negative current period to the boost inductor current. First, the efficiency of the Current-Fed DAB converter is calculated when several operation modes are applied to it.

These several operation modes are classified focused on the boost inductor current mode and secondary voltage levels. Finally, the validity of the proposed method is demonstrated by a 2-kW prototype circuit.

II. CIRCUIT CONFIGURATION

Figure 1 shows the circuit configuration of the Current-Fed DAB converter. This circuit configuration integrates the DC-DC converter into the DAB converter. This circuit achieves a reduction in the number of power conversion stages. Moreover, the capacitor voltage is controlled by the DC-DC converter. Therefore, the transformer voltage ratio matches the turn ratio. Furthermore, the DC-DC converter is a two-phase interleaved configuration. The boost inductor ripple current is reduced by inverting the carrier phase of each phase.

III. OPERATION MODE

Table 1 shows the operation modes for the Current-Fed DAB converter. These operation modes are classified according to the boost inductor current mode and secondary voltage levels. In this circuit, the duty ratio of the power devices on the primary H-bridge fluctuates by the capacitor voltage control. The primary H-bridge is operated as the three-level mode including a zero-voltage period in order to prevent the DC-bias magnetization of the transformer. On the other hand, the secondary H-bridge has two degrees of freedom of two-level mode or three-level mode.

On the other hand, the Current-Fed DAB converter has several current modes of CCM, Discontinuous Current Mode (DCM), and TCM for the boost inductor current. In this section, the transformer RMS current and the ZVS range are discussed in several operation modes. Note that the ZVS operation is achieved when the current flows in the discharge direction of the parasitic capacitance of the power devices and pulls out the charge. This paper focuses only on the current direction of the power device when the ZVS operation is discussed. Therefore, the current magnitude required to pull the charge out of the parasitic capacitance of the power devices is not considered. Moreover, the transformer primary current and the ZVS range in each operation mode are different with the boundary of the condition where the duty ratio of the lower arm power devices on the primary H-bridge is 50% (D=0.5). In this paper, the condition of D>0.5 is discussed because the condition of D<0.5 is considered in the same way. Note that the duty ratio of the lower arm power devices on the primary H-bridge is defined as

$$D = \frac{NV_{out} - V_{in}}{NV_{out}} \quad \text{.....(1)},$$

where N is the turn ratio of the transformer, V_{in} is the input voltage, and V_{out} is the output voltage.

A. Conventional two-level mode

Figure 2(a) shows the operation waveform of the conventional two-level mode. In this operation mode, the

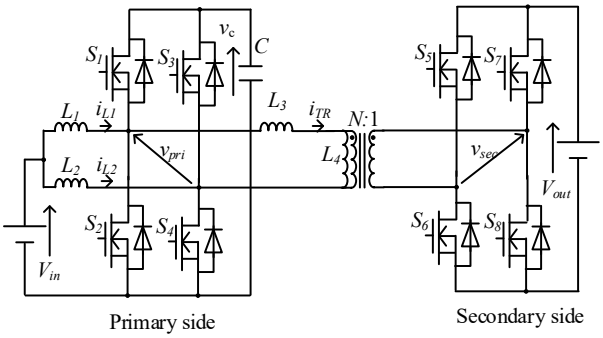

Fig. 1 Circuit configuration of Current-Fed DAB converter. This circuit is the configuration of integrating the primary H-bridge of the DAB converter and the interleave DC-DC converter.

Table. 1 Operation modes for the Current-Fed DAB converter.

	Secondary voltage levels : v_{sec}	Current mode of boost inductor :$i_{L1,L2}$
Conventional two-level mode	two-level	CCM
ZVS range extension two-level mode	two-level	**TCM**
Conventional three-level mode	**three-level**	CCM
ZVS range extension three-level mode(proposed method)	**three-level**	**TCM**

CCM of the boost inductor current is combined with the two-level mode of the secondary H-bridge. This operation mode is a constant switching frequency operation and has six switching modes for one switching cycle. Note that the transformer current is an AC waveform. Therefore, the transformer RMS current is calculated by analyzing half cycle. Thus, the transformer RMS current is expressed as

$$I_{TR\_RMS} = \frac{NV_{out}}{2L_3\omega}\sqrt{\frac{\pi^2(2D-1)^3}{3} - 2(D-1)(2\delta - \pi(2D-1))^2}$$

.....(2),

where δ is the phase shift angle, ω is the angular frequency. In this operation mode, the transformer RMS current increases at light load. The reason for this problem is that the reactive current ratio increases compared to the active current that transmits the power.

Next, the ZVS operation is discussed. The ZVS operation of the power devices on the secondary H-bridge is considered from the transformer current as with the DAB converter. In of the power devices on the secondary H-bridge, transformer current flows in the discharge direction of the parasitic capacitance of the power devices during turn-on. Therefore, the ZVS operation is always achieved when the input voltage variation occurs. On the other hand, the transformer current and the boost inductor current flow into the primary H-bridge. Therefore, the ZVS operation of the power devices on the primary H-bridge is considered from both of these currents. The upper arm power devices on the primary H-bridge always achieve the ZVS

operation due to the boost inductor current at turn-on is the discharge direction of the parasitic capacitance of the power devices. However, the boost inductor current at turn-on flowing through the lower arm on the primary H-bridge is the charge direction of the parasitic capacitance of the power devices. Therefore, the lower arm power devices on the primary H-bridge fail the ZVS operation when the input voltage variation occurs.

B. ZVS range extension two-level mode

Figure 2(b) shows the operation waveform of the ZVS range extension two-level mode. In this operation mode, TCM of the boost inductor current is combined with the two-level mode of the secondary H-bridge. The switching frequency is varied to keep the TCM condition. Moreover, it has six switching modes for one switching cycle, then the transformer RMS current is expressed by (2). In this operation mode, the reactive power increases under light load conditions, and the transformer RMS current increases.

Next, the ZVS operation is discussed. The power devices on the secondary H-bridge always achieve the ZVS operation when the input voltage variation occurs. Moreover, the upper arm power devices on the primary H-bridge always achieve the ZVS operation when the input voltage variation occurs. Furthermore, the lower arm power devices on the primary H-bridge always achieve the ZVS operation due to the boost inductor current at turn-on is the discharge direction of the parasitic capacitance of the power devices.

C. Conventional three-level mode

Figure 3(a) shows the operation waveform of the conventional three-level mode. In this operation mode, the CCM of the boost inductor current is combined with the three-level mode of the secondary H-bridge. This operation mode is a constant switching frequency operation and has eight switching modes for one switching cycle. The transformer RMS current is expressed as

$$I_{TR\_RMS} = \frac{NV_{out}}{\omega L_3}\delta\sqrt{-\frac{\delta}{3\pi}-2(D-1)} \quad \text{.....(3),}$$

In this operation mode, the reactive current does not increase under light load conditions, and the RMS current does not increase.

Next, the ZVS operation is discussed. In this operation mode, the ZVS range is also limited for the power devices on the secondary H-bridge under conditions that $D \neq 0.5$. This is because the transformer current flowing through the power devices during turn-on does not discharge the parasitic capacitance of the power devices. On the other hand, the upper arm power devices on the primary H-bridge always achieve the ZVS operation. Moreover, the lower arm power devices on the primary H-bridge fail the ZVS operation due to the operation with CCM when the input voltage variation occurs.

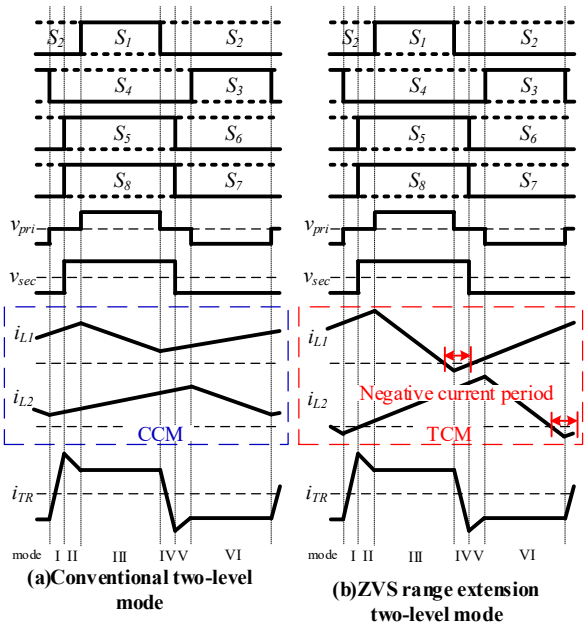

Fig. 2 Operation waveform of two-level mode. The current mode of the boost inductor is CCM in (a). On the other hand, the current mode of the boost inductor is TCM in (b).

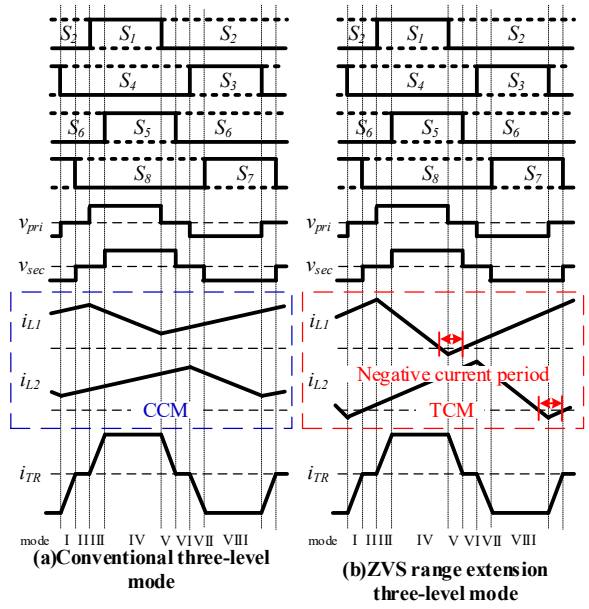

Fig. 3 Operation waveform of three-level mode. The current mode of the boost inductor is CCM in (a). On the other hand, the current mode of the boost inductor is TCM in (b).

D. ZVS range extension three-level mode (proposed method)

Figure 3(b) shows the operation waveform of the proposed ZVS range extension three-level mode. In this operation mode, TCM of the boost inductor current is combined with the three-level mode of the secondary H-bridge. The switching frequency is varied to keep the TCM condition. Moreover, it has eight switching modes for one switching cycle, then the transformer RMS current is expressed by (3). In this operation mode, the

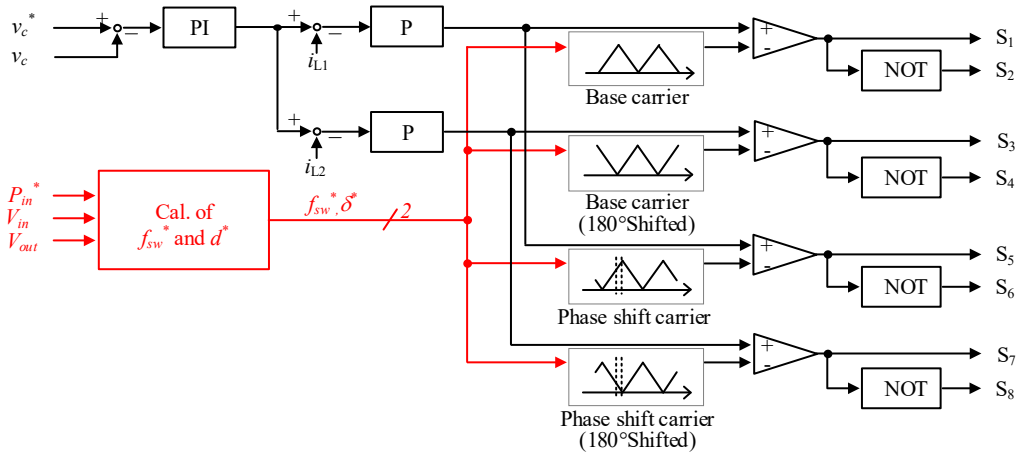

Fig. 4 Proposed control block diagram. This control includes capacitor voltage control, phase shift modulation, and pulse frequency modulation (PFM).

transformer RMS current is the smallest in all operation modes.

Next, the ZVS operation is discussed. The ZVS range is limited for the power devices on the secondary H-bridge under conditions that $D \neq 0.5$. The upper arm power devices on the primary H-bridge always achieve the ZVS operation. Moreover, the power devices on the primary H-bridge always achieve the ZVS operation with TCM when the input voltage variation occurs.

IV. CONTROL SCHEME

Figure 4 shows the proposed control block diagram. In this control, the capacitor voltage is PI-controlled including a boost inductor current P-control. Moreover, the interleaving operation is achieved by the base carrier and the 180 deg. inverted carrier. Furthermore, the transmission power is controlled by the phase shift control. In addition, Pulse Frequency Modulation (PFM) is applied in order to vary the switching frequency. The boost inductor current is always controlled to the TCM by adjusting the ripple current of the boost inductor. The switching frequency is calculated from the boost inductor bottom current and is expressed as

$$f_{sw}^* = \frac{V_{in}}{2(I_{L1,2\_ave}^* + |I_{bottom}|)L_{1,2}} \frac{NV_{out} - V_{in}}{NV_{out}} \quad \text{.....(4),}$$

where f_{sw} is the switching frequency, $I_{L1,2\_ave}$ is the boost inductor average current, I_{bottom} is the boost inductor bottom current, and $L_{1,2}$ is the boost inductor. Note that I_{bottom} is determined to the value required to discharge the parasitic capacitance of the power devices to zero. The phase shift angle is calculated using the power command value, which is expressed as

(when $D > 0.5$)

$$\delta^* = \frac{2\pi}{NV_{out}}(V_{in} - \sqrt{V_{in}^2 - P_{in}^* f_{sw}^* L_3}) \quad \text{.....(5),}$$

(when $D < 0.5$)

$$\delta^* = \frac{2\pi}{NV_{out}}(NV_{out} - V_{in} - \sqrt{(NV_{out} - V_{in})^2 - P_{in}^* f_{sw}^* L_3}) \quad \text{.....(6),}$$

where δ is the phase shift angle and P_{in}^* is the power command value. In this method, the switching frequency and the phase shift angle are calculated and reflected in real-time with the voltage detected values and the power command value. Therefore, the boost inductor current is always controlled to the triangular current mode.

On the other hand, the switching frequency of the Current-Fed DAB converter increases in inverse proportion to the transmission power. Therefore, the switching frequency becomes high under light load conditions and at high input voltage. Therefore, the PFM operation switches to the PWM operation when the switching frequency exceeds the upper limit value f_{sw_lim}. Then, the Current-Fed DAB converter operates by PWM under constant f_{sw_lim} of switching frequency.

On the other hand, there is a PFM method of switching by detecting the zero current of the boost inductor current. In this method, the boost inductor current is controlled to the triangular current mode by switching after detecting the zero current. However, the carrier-based method is applied in this paper because of the ease of switching to PWM at light loads.

V. EFFICIENCY CALCULATION

Table 2 shows the efficiency calculation condition. In this efficiency calculation, only power device losses are considered, magnetic components losses, etc. are not considered. Power device Losses are calculated from switching loss and conduction loss, which is expressed as

$$\begin{aligned} P_{loss} &= P_{cond} + P_{sw} \\ &= I_{RMS}^2 R_{on} + E_{sw} f_{sw} \end{aligned} \quad \text{.....(7),}$$

where P_{loss} is the power device losses, P_{cond} is the conduction loss, P_{sw} is the switching loss, I_{rms} is the current RMS value, R_{on} is the on-resistance, E_{sw} is the switching energy, and f_{sw} is the switching frequency. The on-resistance is referenced from the datasheet, and the RMS value is calculated from the transformer current and the boost inductor current. Moreover, the switching energy is fitted by a linear first-order approximation of the datasheet values. Furthermore, the switching loss at

turn-on is zero at the condition achieving the ZVS operation.

Figure 5 shows the transformer RMS current with input voltage at rated power. In the conventional three-level mode and the conventional two-level mode, the transformer RMS current becomes small compared to that of the DAB converter because the transformer's primary voltage is increasing with the voltage control. Moreover, the transformer RMS current of the ZVS range extension three-level mode becomes the smallest in all operation modes. The smallest transformer RMS current is 5.0A at the input voltage of 300V. The transformer RMS current is reduced by up to 72.3% compared to that of the DAB converter at the input voltage of 150V. However, the transformer RMS current of the ZVS extension two-level mode increases when the input voltage variation occurs because of the increased reactive power by the decreased switching frequency.

Figure 6 shows the calculated efficiency considering only power device losses with the input voltage at rated power. In the conventional three-level mode and the conventional two-level mode, the efficiency of the Current-Fed DAB converter is low compared to that of the DAB converter under high input voltage conditions because of the increased switching loss by the limitation of the ZVS range. In the ZVS extension two-level mode, the efficiency of the Current-Fed DAB converter is greatly reduced when the input voltage variation occurs because of the increased conduction loss by the increased transformer RMS current. On the other hand, the efficiency of the Current-Fed DAB converter with the ZVS range extension three-level mode is the highest in all operation modes against the input voltage variation. The calculated efficiency considering only power device losses of the Current-Fed DAB converter with the ZVS range extension three-level mode is 98.7% at the input voltage of 150V, which is improved by approximately 3.0% compared to that of the DAB converter. In addition, The maximum efficiency is 99.1% at the input voltage of 300V.

VI. EXPERIMENTAL RESULTS

Table 3 shows the experimental conditions. In this section, the validity of the proposed method is demonstrated by the 2-kW prototype.

Figure 7 shows the operation waveform at the input voltage of 200V. According to figure 7(a), the transformer voltage becomes a three-level waveform including a zero voltage period. In addition, the boost inductor current becomes positive with the CCM operation. On the other hand, according to Figure 7(b), the negative current occurs in the inductor current with the TCM operation. Note that The switching frequency is 28kHz. This indicates that the boost inductor current achieves the triangular current mode by adjusting the ripple current with PFM. In addition, according to figure 7(c), the ripple currents and the average currents are equal on each boost inductor current. This indicates that each boost inductor current is balanced.

Figure 8 shows the operation waveform at the input voltage of 450V. According to figure 8(a), the current

Table.2 Efficiency calculation condition.

Element	Symbol	Value
Input power	P_{in}	3 kW
Switching frequency	f_{sw}	(DAB)50 kHz
		(conventional mode) 300kHz(two-level), 200 kHz(three-level)
		(ZVS range extension mode) 10-300 kHz
Input voltage	V_{in}	150-450 V
Output voltage	V_{out}	300 V
Turn ratio	N	(DAB)N_1:N_2=1:1
		(Current-fed DAB)N_1:N_2=2:1
Leakage inductor	L_3	37.5 μH
Boost inductor	L_1,L_2	(DAB)-
		(Current-Fed DAB)500 μH
Magnetizing inductance	L_4	6 mH
Capacitor	C	650 μF
MOS FET		SCT3040KL

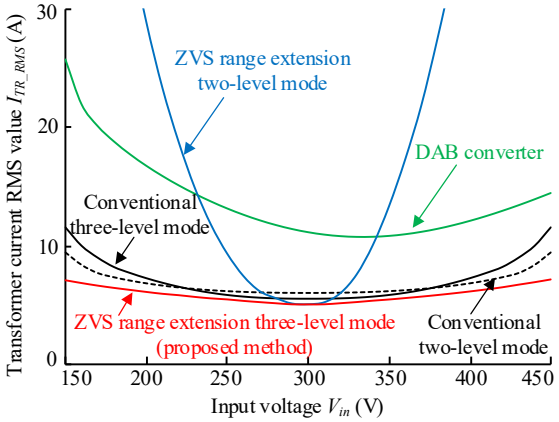

Fig. 5 Transformer RMS current with input voltage at rated power. The transformer RMS current of the Current-Fed DAB converter with the proposed method is the lowest in all operation modes.

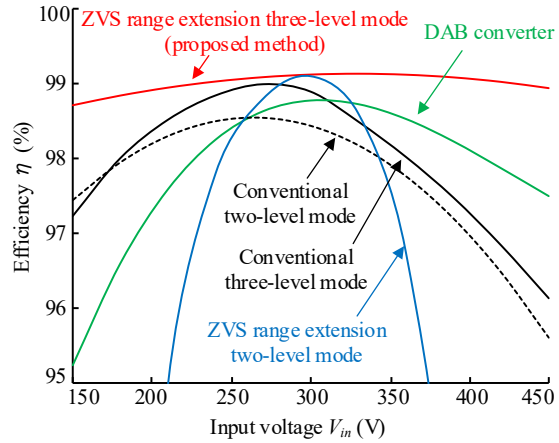

Fig. 6 Efficiency with input voltage at rated power. The efficiency of the Current-Fed DAB converter with the proposed method is the highest in all operation modes.

Table3. Experimental condition.

Element	Symbol	Value
Input power	P_{in}	2 kW
Switching frequency	f_{sw}	(Conventional three-level mode) 100 kHz
		(ZVS range extension three-level mode)18-100 kHz
Input voltage	V_{in}	150-450 V
Output voltage	V_{out}	300 V
Turn ratio	N	N_1:N_2=2:1
Leakage inductor	L_3	105 μH
Boost inductor	L_1,L_2	390 μH
Magnetizing inductance	L_4	6 mH
Capacitor	C	650 μF
Dead-time	T_d	125ns
MOS FET		SCT3040KL

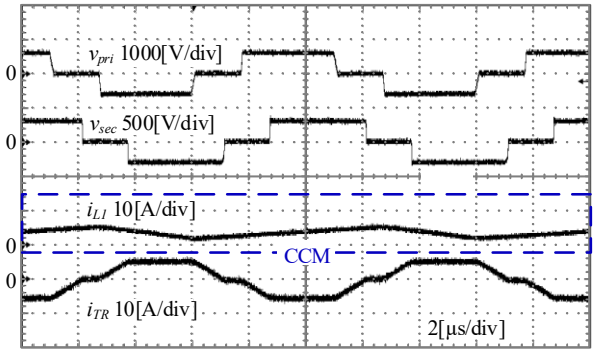

(a) Conventional three-level mode

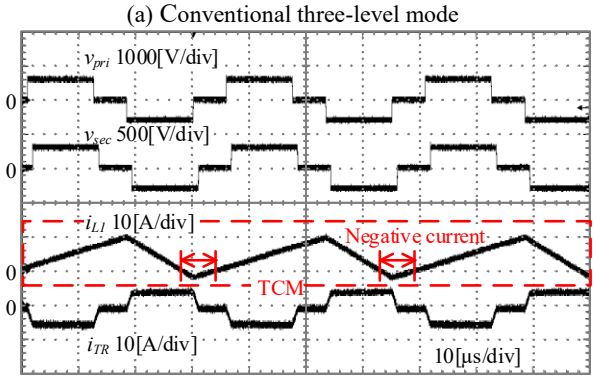

(b)ZVS range extension three-level mode

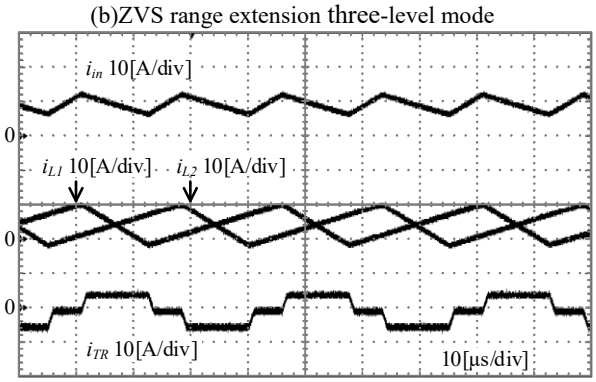

(c) Balanced waveform of each boost inductor current

Fig.7 Experimental waveform at the input voltage of 200V. The mode of i_{L1} is the CCM in (a). On the other hand, the mode of i_{L1} is the TCM in (b). In addition, i_{L1} and i_{L2} are balanced in (c).

mode of boost inductor is CCM. According to figure 8(b), the current mode of boost inductor is TCM. Note that the

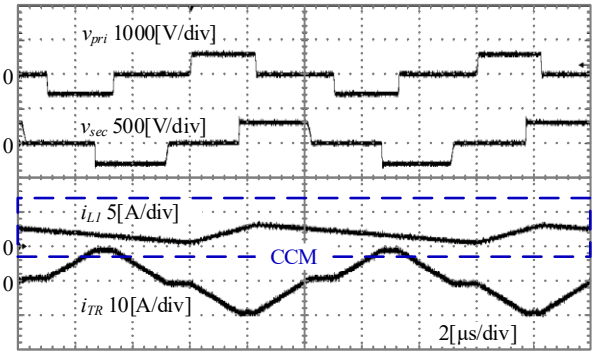

(a)Conventional three-level mode

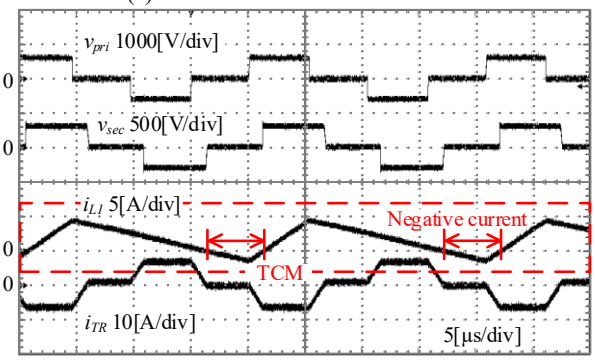

(b)ZVS range extension three-level mode

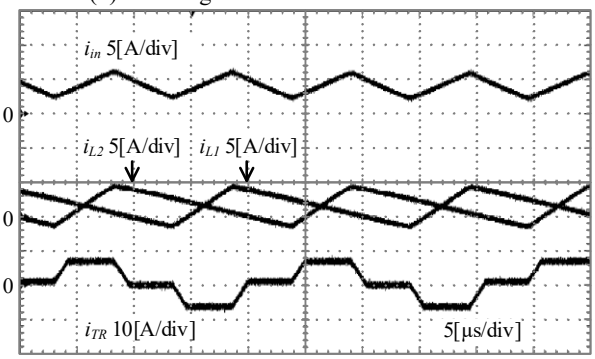

(c) Balanced waveform of each boost inductor current

Fig.8 Operation waveform at the input voltage of 450V. The mode of i_{L1} is the CCM in (a). On the other hand, the mode of i_{L1} is the TCM in (b). In addition, i_{L1} and i_{L2} are balanced in (c).

switching frequency is 45kHz. In addition, figure 8(c) indicates that each boost inductor current is balanced.

Figure 9 shows the switching waveform of S_2 at the input voltage of 450V. In the conventional three-level mode shown in figure 9(a), the drain-source voltage is still applied when the gate-source voltage is applied. This indicates that the S_2 current during the dead time flows in the charging direction of the parasitic capacitance of the power devices. Therefore, S_2 of the conventional three-level mode operates with hard-switching at turn-on. In the ZVS range extension three-level mode shown in figure 9(b), the drain-source voltage is zero when the gate-source voltage is applied. This indicates that the S_2 current during the dead time flows in the discharging direction of the parasitic capacitance of the power devices. Therefore, S_2 of the ZVS range extension three-level mode is achieve ZVS operation at turn-on.

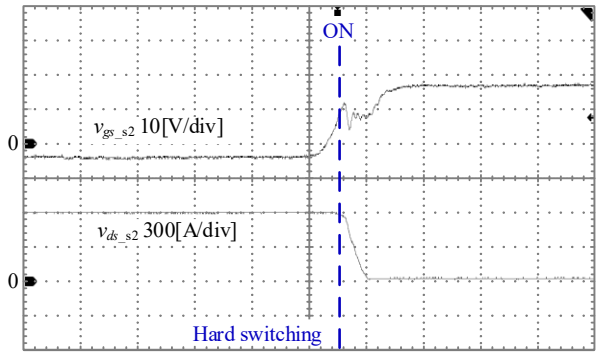

(a)Conventional three-level mode

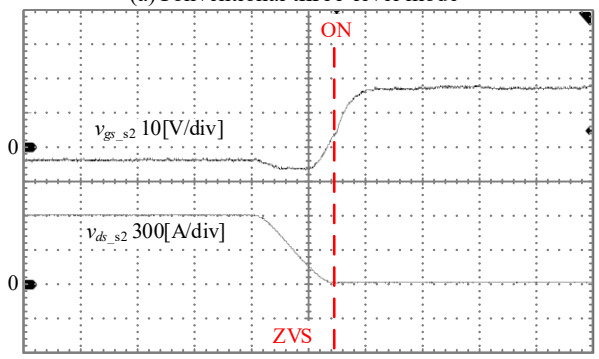

(b)ZVS range extension three-level mode

Fig.9 Switching waveform of S_2 at the input voltage of 450V. In (a), the ZVS operation fails at turn-on. On the other hand, in (b), ZVS operation is achieved at turn-on.

Figure 10 shows the efficiency with input voltage at rated power. The efficiency of the Current-Fed DAB converter with the conventional three-level mode is 97.3% at the input voltage of 300V. However, the efficiency is 94.1% at the input voltage of 450V, which indicates that the efficiency is drastically decreased when the input voltage variation occurs. On the other hand, the efficiency of the Current-Fed DAB converter with the ZVS range extension three-level mode is 97.5% at the input voltage is 300V. Moreover, the efficiency is 97.2% at the input voltage of 450V, which indicates that the high-efficiency operation is achieved against the input voltage variation. Furthermore, the efficiency of the Current-Fed DAB converter with the ZVS range extension three-level mode improved by 3.1% compared to that of the conventional three-level mode when the input voltage is 450V. This indicates that the loss of the Current-Fed DAB converter is reduced by 52.5% compared to that of the conventional method.

Figure 11 shows the efficiency with transmission power. At the input voltage of 150 V in figure 11(a), the efficiency of the ZVS extension three-level mode is higher than the conventional three-level mode under all load conditions. In addition, the efficiency is improved by 1.6% at the rated power. At the input voltage of 450 V in figure 11(b), the efficiency of the ZVS extension three-level mode is also higher than the conventional three-level mode under all load conditions. In addition, the efficiency is improved by 3.1% at the rated power.

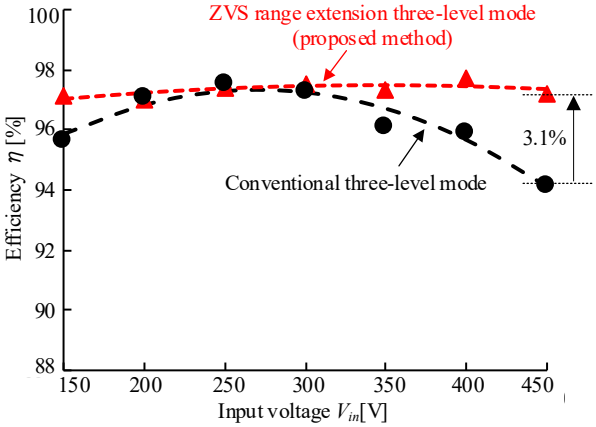

Fig.10 Efficiency with input voltage at rated power. The efficiency of the Current-Fed DAB converter with the proposed method improved by 3.1% compared to that of the conventional three-level mode at the input voltage of 450V.

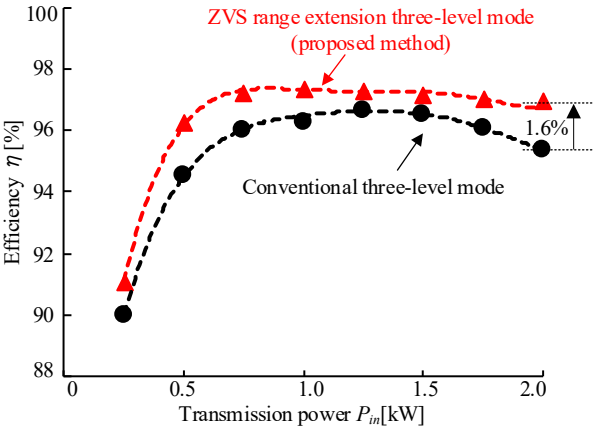

(a)Input voltage of 150V

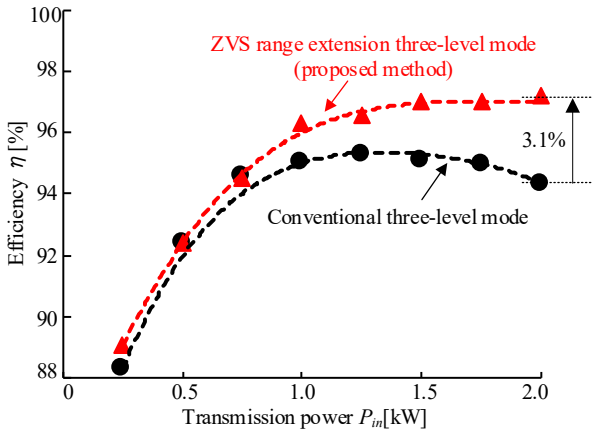

(b)Input voltage of 450V

Fig.11 Efficiency with transmission power. The efficiency of the Current-Fed DAB converter with the proposed method is improved over a wide load range compared to that of the conventional three-level mode.

VII. CONCLUSIONS

This paper proposed the control method improving the efficiency of the Current-Fed DAB converter against the input voltage variation. The proposed method with PFM always controls the boost inductor current to TCM by changing the switching frequency when the input voltage variation occurs. Therefore, the ZVS range of power devices was extended with the TCM operation of the boost inductor current.

The validity of the proposed method was demonstrated by a 2-kW prototype circuit. As a result, the maximum efficiency of the Current-Fed DAB converter in the proposed method is 97.5% at rated load conditions. Moreover, the efficiency of the Current-Fed DAB converter with the proposed method was 97.2% when the input voltage was varied by 50% from the nominal condition, then the loss was reduced by 52.5% compared to that of the conventional method. The future work is loss separation considering iron loss and power density evaluation.

REFERENCES

[1] N. Hatziargyriou, H. Asano, R. Iravani, C. Marnay: "Microgrids", IEEE Power Energy Mag, Vol. 6, No. 3, pp. 78-94 (2008).

[2] H. Kakigano, Y. Miura, and T. Ise, "Low-Voltage Bipolar-Type DC Microgrid for Super High Quality Distribution", IEEE Transactions on Power Electronics, Vol. 25, No. 12, pp. 3066-3075 (2010).

[3] D. Segaran, D. G. Holmes, B. P. McGrath: "Enhanced load step response for a bidirectional dc-dc converter", IEEE Transactions on Power Electronics, Vol. 28, No. 1, pp. 371-379 (2013).

[4] K. Takagi, H. Fujita: "Dynamic Control and Performance of a Dual-Active-Bridge DC–DC Converter", IEEE Transactions on Power Electronics, Vol. 33, No. 9, pp. 7858-7866 (2018).

[5] L. Jin, B. Liu, S. Duan: "ZVS operation range analysis of three-level dual active bridge DC-DC converter with phase-shift control", 2017 IEEE Applied Power Electronics Conference and Exposition, pp. 362-366(2017)

[6] M. N. Kheraluwala, R. W. Gascoigne, D. M. Divan, E. D. Baumann: "Performance Characterization of a High Power Dual Active Bridge dc-to-dc Converter", IEEE Transactions on Industry Applications, Vol. 28, No. 6, pp. 1294-1301(1992).

[7] T. Mishima, Y. Koga: "Variable Frequency Phase-Shift Modulation Symmetrical Series-Resonant Bidirectional DC-DC Converter-Analysis and Verification of ZVS Performance and Reactive Power Minimization-", IEEJ Journal of Industry Applications, Vol. 10, No. 5, pp. 540-553(2021).

[8] R. Kondo, Y. Higaki, M. Yamada: "Experimental Verification of Reducing Power Loss under Light Load Condition of a Bi-Directional Isolated DC/DC Converter for a Battery Charger-Discharger of Electric Vehicle", IEEJ Journal of Industry Applications, Vol. 10, No. 3, pp. 377-383(2021).

[9] Y. Tashiro, H. Haga: "Improvement of Light-Load Efficiency by using a Six-Arm Converter with Series-Parallel Switching", IEEJ Journal of Industry Applications, Vol. 10, No. 2, pp. 273-281(2021).

[10] S. Inoue, K. Itoh, M. Ishigaki, T. Sugiyama: "Integrated Magnetic Component of a Transformer and a Magnetically Coupled Inductor for a Three-Port DC-DC Converter", IEEJ Journal of Industry Applications, Vol. 9, No. 6, pp. 713-722(2020).

[11] K. Sun, Y. Gao, H. Chen: "Bi-Directional High-Conversion-Ratio CLLC Resonant Converter with a New Synchronous Rectification Scheme for Low Conduction Loss", IEEJ Journal of Industry Applications, Vol. 9, No. 5, pp. 515-522(2020).

[12] P. A. M. Bezerra, F. Krismer, R, M. Burkart, J. W. Kolar: "Bidirectional Isolated Non-Resonant DAB DC‑DC Converter for Ultra-Wide Input Voltage Range Applications", 2014 International Power Electronics and Application Conference and Exposition (2014)

[13] A. K. Jain, R. Ayyanar, "Pwm control of dual active bridge: Comprehensive analysis and experimental verification", IEEE Transactions on Power Electronics, vol. 26, no. 4, pp. 1215-1227 (2011)

[14] R. M. Burkart, J. W. Kolar: "Comparative Efficiency-power density-costs Pareto Optimization of Si and SiC Multi-Level Dual Active Bridge Topologies with Wide Input Voltage Range", IEEE Transactions on Power Electronics, Vol.32, No.7, pp.5258-5270 (2017)

[15] H. Hayato, J. Itoh: "Development of T-type Dual Active Bridge DC-DC Converter with Switching Operation Mode Over Wide-Voltage-Operation Range", IEEJ Journal of Industry Applications, Vol. 139, No. 4, pp. 388-400 (2019)

[16] M. Soleimanifard, A. Y. Varjani: "A Bidirectional Buck-Boost Converter in Cascade with a Dual Active Bridge Converter to Increase the Maximum Input and Output Currents and Extend Zero Voltage Switching Range", 2020 11th Power Electronics, Drive Systems, and Technologies Conference (2020)

[17] J. Guo, H. Han, G. Xu, Z. Cai, H. Wang, Y. Sun, M. Su: "Design Considerations for PPS Controlled Current-Fed DAB Converter to Achieve Full Load Range ZVS with Low Inductor RMS Current", 2020 IEEE Energy Conversion Congress and Exposition (ECCE), pp. 5971-5975(2020)

[18] A. Pal, S. Kapat: "Accurate Discrete-Time Modeling of an Interleaved Current-Fed Dual Active Bridge DC-DC Converter", 2019 IEEE Applied Power Electronics Conference and Exposition, pp. 1616-1621 (2016).

[19] Y. Shi, R. Li, Y. Xue, H. Li: "Optimized Operation of Current-Fed Dual Active Bridge DC–DC Converter for PV Applications" IEEE Transactions on Industrial Electronics, Vol. 62, No. 11, pp. 6986-6995 (2015)

[20] M. Han, X. Liu, L. Zhao, K. Wang, Y. Yao, D. Xu: "Sliding Mode Control Based on a Linear Quadratic Regulator for Current-Fed Dual Active Bridge Converter", 2019 22nd International Conference on Electrical Machines and Systems (2019)

[21] Z. Guo, K. Sun, T. Wu, C. Li: "An Improved Modulation Scheme of Current-Fed Bidirectional DC–DC Converters For Loss Reduction", IEEE Transactions on Power Electronics, Vol. 33, No. 5, pp. 4441-4457 (2018)